

A Study on the Development of Chemical Vapor Deposition Precursors. 4. Syntheses and Characterization of New *N*-Alkoxo- β -ketoiminate Complexes of Niobium and Tantalum

Sunkwon Lim, Joong Cheol Lee, Do Sung Sohn, Wan In Lee,^{*,†} and Ik-Mo Lee^{*,‡}

Department of Chemistry, Inha University, 253 Yonghyundong, Namku, Incheon 402-751, Korea

Received June 19, 2001. Revised Manuscript Received February 12, 2002

Partial replacement of ethoxide ligands with *N*-alkoxo- β -ketoiminates in the tantalum or niobium ethoxides resulted in $M(N\text{-alkoxo-}\beta\text{-ketoiminate})(\text{OEt})_3$ ($M = \text{Ta}$ and Nb) complexes. Most of these complexes are liquid and showed enhanced thermal and chemical stability, especially toward moisture. These complexes have octahedral geometry with a meridional *N*-alkoxo- β -ketoiminate ligand and showed fluxional behaviors. All of these precursors, especially the ones with methyl groups on both the *N*-alkoxo and β -ketoiminate backbones, demonstrate considerably higher deposition rates than $M_2(\text{OEt})_{10}$ ($M = \text{Ta}$ and Nb), one of the most popular precursors for Ta_2O_5 and Nb_2O_5 films. Thermogravimetric analysis experiments showed that successive decomposition of ethoxide ligands is followed by decomposition of *N*-alkoxo- β -ketiminate in the pyrolysis process. Introduction of a methyl group onto the *N*-hydroxyethyl backbone enhanced the thermal stability at lower temperatures and the pyrolysis rate at higher temperatures. X-ray diffraction patterns indicate that the deposited films are not crystallized until the substrate temperature goes over 650 °C. Well-crystallized longish grains were formed in the Ta_2O_5 film deposited at 700 °C, but it was found from the depth profile spectra by Auger electron spectroscopy (AES) that the nitrogen and carbon impurities are 2.3% and 4.2%, respectively, for the Ta_2O_5 film deposited at 550 °C. Heat treatment at 700 °C in oxygen removed the nitrogen impurity in this Ta_2O_5 completely, and the residual carbon was proved to be negligible from the AES and X-ray photoelectron spectroscopy results.

Introduction

Group 5 metal oxides, especially Nb_2O_5 and Ta_2O_5 , have drawn much interest because of important applications. Tantalum oxide, Ta_2O_5 , has drawn much interest because of its highest dielectric constant among the single metal oxides, which have promising applications as dielectric materials in high-density dynamic random access memories, integrated optical devices, thin film capacitors, large-scale integration, electroluminescent devices,¹ and solid-state ion sensors.² The recent discovery of enhancement of the dielectric constant and crystallization temperature of Ta_2O_5 by addition of a small amount of various metal oxides may induce wider applications.³ In addition, layered perovskite materials containing tantalum oxides such as SBT ($\text{SrBi}_2\text{Ta}_2\text{O}_9$) have been considered as capacitor materials for ferroelectric-based memory devices (FeRAMs).⁴ Materials containing tantalum oxides such as BMT

[$\text{Ba}(\text{Mg}_{1/3}\text{Ta}_{2/3})\text{O}_3$] and BZT [$\text{Ba}(\text{Zn}_{1/3}\text{Ta}_{2/3})\text{O}_3$] have attractive microwave dielectric properties and are considered to be archetypal high- Q dielectric resonator materials.⁵

Nb_2O_5 is a dielectric material applicable in capacitor technology, waveguides, oxygen sensors, and corrosion-resistant and electrochromic coatings.⁶ Also lithium niobate (LiNbO_3) and $\text{Pb}(\text{Mg},\text{Nb})\text{O}_3$ containing Nb_2O_5 are known to have excellent ferroelectric and piezoelectric properties and large electrooptic and nonlinear optical coefficients.^{7,8}

To prepare thin films containing Ta_2O_5 or Nb_2O_5 by metalloorganic chemical vapor deposition (MOCVD)

* To whom correspondence should be addressed. Fax: +82-32-867-5604.

[†] E-mail: wanin@inha.ac.kr.

[‡] E-mail: imlee@inha.ac.kr.

(1) (a) Pollard, K. D.; Puddephatt, R. J. *Chem. Mater.* **1999**, *11*, 1069–1074 and references therein. (b) Chaneliere, C.; Autran, J. L.; Devine, R. A. B.; Balland, B. *Mater. Sci. Eng.* **1998**, *R22*, 269–322. (c) Treichel, H.; Mitwalsky, A.; Sandler, N. P.; Tribula, D.; Kern, W.; Lane, A. P. *Adv. Mater. Opt. Electron.* **1992**, *1*, 299.

(2) Teravaninthorn, U.; Miyahara, Y.; Moriizumi, T. *Jpn. J. Appl. Phys.* **1987**, *26*, 2116.

(3) (a) Cava, R. F.; Peck, W. F., Jr.; Krajewski, J. J. *Nature* **1995**, *377*, 215. (b) Cava, R. F.; Krajewski, J. J. *J. Appl. Phys.* **1998**, *83*, 1613. (c) Cava, R. F.; Peck, W. F., Jr.; Krajewski, J. J.; Roberts, G. L.; Barber, B. P.; O'Bryan, H. M.; Gammel, P. L. *Appl. Phys. Lett.* **1997**, *70*, 1396. (d) van Dover, R. B.; Fleming, R. M.; Schneemeyer, L. F.; Alers, G. B.; Werder, D. J. *Tech. Dig.-Int. Electron Devices Meet.* **1998**, 823.

(4) Roeder, J. F.; Hendrix, B. C.; Hintermaier, F.; Desrochers, D. A.; Baum, T. H.; Bhandari, G.; Chappuis, M.; Van Buskirk, P. C.; Dehm, C.; Fritsch, E.; Nagel, N.; Wendt, H.; Cerva, H.; Honlein, W.; Mazure, C. *J. Eur. Ceram. Soc.* **1999**, *19*, 1463–1466.

(5) Ra, S. H.; Phule, P. P. *J. Mater. Res.* **1999**, *14*, 4259.

(6) Kukli, K.; Ritala, M.; Leskelä, M.; Lappalainen, R. *Chem. Vap. Deposition* **1998**, *4*, 29–34.

(7) (a) Lee, S. Y.; Feigelson, R. S. *J. Mater. Res.* **1999**, *14*, 2662. (b) Weis, R. S.; Gaylord, T. K. *Appl. Phys.* **1985**, *A37*, 191.

(8) Jones, A. C.; Leedham, T. J.; Wright, P. J.; Crosbie, M. J.; Williams, D. J.; Lane, P. A.; O'Brien, P. *Mater. Res. Soc. Symp. Proc.* **1998**, *495*, 11.

processes, a variety of Ta precursors such as $Ta_2(OR)_{10}$ ($R = Me$ and Et), $[Ta(dpm)_4Cl]$ ($dpm = 2,2,6,6$ -tetramethyl-3,5-heptanedionato), $[TaMe_3(OR)_2]$ ($R = C_{2-7}$ alkyl groups), $[Ta(NMe_2)_5]$, $[TaX_5]$ ($X = Cl, F$), $[TaCl_2(OEt)_2(acac)]$ ($acac = acetylacetonate$), $[Ta(OR)_4(\beta\text{-diketonate})]$, $[Ta(dmae)(OEt)_4]$ [$dmae = (N,N\text{-dimethylamino})\text{-ethanolate}$], liquid mixture, containing $(Et_3N)_3Ta=NEt$ and $(Et_3N)_3Ta(\eta^2\text{-EtN=CHMe})$, and Nb precursors such as $[Nb(OR)_5]_2$, $[Nb(dmae)(OEt)_4]$, $[Nb(dpm)_2Cl_3]$, and $Nb(dpm)_4$ have been exploited.^{1,6,8,9}

Because of the requirement of low-temperature film deposition for integrated circuit applications, various methods such as plasma-enhanced MOCVD,¹⁰ water-assisted CVD,¹¹ and atomic layer deposition (ALD)¹² have been adopted. In these processes, the most commonly used metal alkoxides, $M_2(OR)_{10}$ ($M = Nb$ and Ta), are prone to being hydrolyzed. However, substitution of alkoxide ligands with chelating $\beta\text{-diketonate}^{1a}$ or "donor-functionalized" alkoxide ligands⁸ resulted in much reduced moisture sensitivity. The same phenomenon was observed in similar titanium complexes.¹³

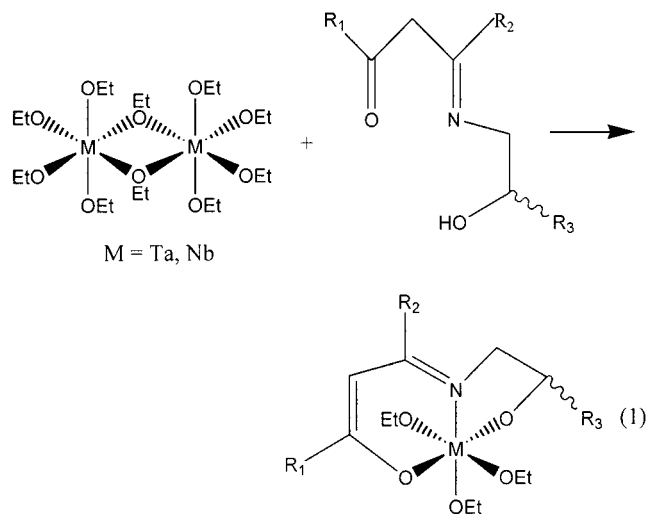
Recently, $\beta\text{-ketoiminate}$ complexes have drawn interest because of their higher thermal stability than the $\beta\text{-diketonate}$ analogues and their versatility, by changing the imine substituents, for tailoring their reactivity and volatility.^{14,15} Several $\beta\text{-ketoiminates}$ and fluorinated $\beta\text{-ketoiminates}$ of Cu, Ni, Ag, Ba, and Pd have been successfully used as precursors for metal or metal oxide deposition.¹⁶ In addition, several polydentate ligands have been exploited for the saturation of the coordination spheres to increase volatility and chemical and thermal stability¹⁷ in the alkaline-earth metal¹⁸ and lead precursors.¹⁹

The terdentate dianionic nature of the $N\text{-alkoxo-}\beta\text{-ketoiminate}$ ligands is expected to show enhanced stability and volatility by combination of increased saturation and chelate effect, while the high oxidation state of a metal center such as +5 can be maintained with fewer ligands. With this in mind, reactions between $M_2(OEt)_{10}$ ($M = Nb$ and Ta) and $N\text{-alkoxo-}\beta\text{-ketoiminate}$ were carried out to produce $M(N\text{-alkoxo-}\beta\text{-ketoiminate})(OEt)_3$. Also, the substituent effect on the properties of these complexes and potential availability as MOCVD

precursors to tantalum or niobium oxides have been studied in this paper.

Results and Discussion

The Ta and Nb complexes were prepared from the substitution reaction between $Ta_2(OEt)_{10}$ or $Nb_2(OEt)_{10}$ and appropriate $N\text{-alkoxo-}\beta\text{-ketoimine}$ (eq 1). The yields



2a;	$R_1 = Me, R_2 = Me, R_3 = H$
2b;	Me, Me, Me
2c;	i-Pr, i-Pr, H
2d;	i-Pr, i-Pr, Me
2e;	t-Bu, Me, H
3a;	Me, Me, H
3b;	Me, Me, Me
3c;	i-Pr, i-Pr, H
3d;	i-Pr, i-Pr, Me

were found to be dependent on the reaction temperature; at room temperature, they were moderate (around 60%), but slight heating to around 35 °C induced much higher yields (over 90%). The products were characterized by 1H and ^{13}C NMR, thermogravimetric analysis/differential scanning calorimetry (TGA/DSC), and elemental analyses.

(9) Senzaki, Y.; Hochberg, A. K.; Norman, J. A. *Adv. Mater. Opt. Electron* **2000**, *10*, 93–103.

(10) Nagahori, A.; Raj, R. *J. Am. Ceram. Soc.* **1995**, *78*, 1585.

(11) Li, X.; Hitchman, M. L.; Shamlian, S. H. *Electrochem. Soc. Proc.* **1997**, *97–25*, 1246.

(12) (a) Kukli, K.; Ritala, M.; Leskela, M. *Chem. Mater.* **2000**, *12*, 1914. (b) Kukli, K.; Aarik, J.; Aidla, A.; Forsgren, K.; Sundqvist, J.; Harsta, A.; Uustare, T.; Mandar, H.; Kilsler, A.-A. *Chem. Mater.* **2001**, *13*, 122.

(13) (a) Hong, S. T.; Lim, J. T.; Lee, J. C.; Xue, M.; Lee, I. M. *Bull. Korean Chem. Soc.* **1996**, *17*, 637–642. (b) Jones, A. C.; Ledham, T. J.; Wright, P. J.; Crosbie, M. J.; Fleeting, K. A.; Otway, D. J.; O'Brien, P.; Pemble, M. E. *J. Mater. Chem.* **1998**, *8*, 1773.

(14) Bastianini, A.; Battiston, G. A.; Benetollo, F.; Gerbasi, R.; Porchia, M. *Polyhedron* **1997**, *16*, 1105–1110.

(15) Doherty, S.; Errington, R. J.; Housley, N.; Ridland, J.; Clegg, W.; Elsegood, M. R. *J. Organometallics* **1999**, *18*, 1018–1029 and references therein.

(16) (a) Shin, H. K.; Hampden-Smith, M. J.; Kostas, T. T.; Rheingold, A. L. *J. Chem. Soc., Chem. Commun.* **1992**, 217. (b) Gerfin, T.; Bechi, M.; Dahmen, K. H. *Mater. Sci. Eng.* **1993**, *B17*, 97. (c) Bechi, M.; Galhts, J.; Huaziker, M.; Ataniny, F.; Dahmen, K. H. *J. Phys., Colloq.* **1995**, *C5*, 465. (d) Schulz, D. L.; Hinds, B. J.; Stern, C. L.; Marks, T. J. *Inorg. Chem.* **1993**, *32*, 249. (e) Edwards, D. A.; Harker, R. M.; Mahon, M. F.; Molloy, K. C. *J. Mater. Chem.* **1999**, *9*, 1771–1780. (f) Zhang, Y.; Yuan, Z.; Puddephatt, R. J. *Chem. Mater.* **1998**, *10*, 2293–2300. (g) Tung, Y.-L.; Tseng, W.-C.; Lee, C.-Y.; Hsu, P.-F.; Chi, Y.; Peng, S.-M.; Lee, G.-H. *Organometallics* **1999**, *18*, 864–869.

(17) (a) Fujinaga, T.; Kuwamoto, T.; Maurai, S. *Talanta* **1971**, *18*, 429. (b) Fujinaga, T.; Kuwamoto, T.; Maurai, S. *Anal. Chim. Acta* **1974**, *71*, 141. (c) Fujinaga, T.; Kuwamoto, T.; Sugiura, K.; Ichiki, S. *Talanta* **1981**, *28*, 295. (d) Fujinaga, T.; Kuwamoto, T.; Sugiura, K.; Matsubara, N. *Anal. Chim. Acta* **1982**, *136*, 175. (e) Dickinson, P. H.; Geballe, T. H.; Sanjurjo, A.; Hildenbrand, D.; Craig, G.; Zisk, M.; Collman, J.; Banning, S. A.; Sievers, R. E. *J. Appl. Phys.* **1989**, *66*, 444. (f) Timmer, K.; Spee, C. I. M. A.; Mackor, A.; Meinema, H. A. European Patent Appl. 0405634A2, 1991. (g) Barron, A. R.; Buriak, J. M.; Cheatham, L.; Gordon, R. The Electrochemical Society 177th Meeting, Montreal, Canada, 1990; Abstract 943 HTS. (h) Gardiner, R.; Brown, D. W.; Kirilin, P. S.; Rheingold, A. L. *Chem. Mater.* **1991**, *3*, 1053. (i) Malandrino, G.; Richeson, D. S.; Marks, T. J.; DeGroot, D. C.; Schindler, J. L.; Kannewurf, C. R. *Appl. Phys. Lett.* **1991**, *58*, 182. (j) Gardiner, R. A.; Gordon, D. C.; Stauff, G. T.; Vaartstra, B. A.; Ostrander, R. L.; Rheingold, A. L. *Chem. Mater.* **1994**, *6*, 1967. (k) Kimura, T.; Yamauchi, H.; Machida, H.; Kokubun, H. *Jpn. J. Appl. Phys.* **1994**, *33*, 5119.

(18) (a) Rees, W. S., Jr.; Dippel, K. A. In *Chemical Processing of Advanced Materials*; Hench, L. H., Ed.; Wiley: New York, 1992. (b) Rees, W. S., Jr.; Moreno, D. A. *J. Chem. Soc., Chem. Commun.* **1991**, 1759. (c) Rees, W. S., Jr.; Caballero, C. R.; Hesse, W. *Angew. Chem., Int. Ed. Engl.* **1992**, *31*, 735. (d) Schulz, D. L.; Hinds, B. J.; Stern, C. L.; Marks, T. J. *Inorg. Chem.* **1993**, *32*, 249.

(19) Lim, J. T.; Lee, J. C.; Lee, W. I.; Lee, I. M. *Bull. Korean Chem. Soc.* **1999**, *20*, 355.

These complexes were found to be in the liquid phase or easy melting solids at ambient conditions. They are thermally stable enough to be purified by vacuum distillation and showed enhanced stability toward hydrolysis, as expected. The same phenomenon was reported in the Ta,^{1a,8} Ti,²⁰ and Zr complexes²¹ containing β -diketonates. The reduced chance of alkoxide decomposition induced by decreasing the number of alkoxide ligands may help this enhanced moisture stability. These complexes did not show any indication of decomposition after 2 days in air. However, NMR experiments showed that these complexes exchanged ligands with external EtOH or H₂O slowly and that the exchange rate increased with temperature. On the other hand, Ta(OEt)₄(acac) (acac = acetylacetonate), one of the best known Ta₂O₅ precursors, is known to be air-sensitive and reacted immediately with H₂O.

Generally, Nb complexes showed less sensitivity to hydrolysis than the corresponding Ta ones. This is rather unexpected from the viewpoint of the similar size of Nb(V) and Ta(V).²² More stable hydrolysis products due to stronger M–L bonds with going down in a triad may be the reason.

Analysis of the ¹H and ¹³C NMR spectra of the metal complexes confirmed the *Oh* structure with a meridional distribution of the alkoxide ligands as reported in the complexes of Ti and Nb.¹¹ These complexes show fluxional behaviors. Detailed study on this behavior is in progress.

The TGA data for these complexes are summarized in Table 1 (Supporting Information). This clearly shows that pyrolysis of these complexes begins with the decomposition of the ethoxide ligands one by one. The residue weight percents for all complexes at 100, 150, and 200 °C are almost equal to the theoretical values for fragments where one, two, and three ethoxide ligands are removed from the initial complexes. If only sublimation caused the observed weight loss, the declining line should be linear and the residue amounts virtually become nearly zero. In fact, the slopes are usually steep at the early stage but remain smooth or plateau-like at the later stage. The pyrolysis of the remaining *N*-alkoxy- β -ketoiminate ligand is believed to start at the O-coordinated fragments because the X-ray photoelectron spectroscopy (XPS) data of the thin films deposited by using complexes with these ligands showed that some nitrogen impurities were present.

From the isothermal TGA data, it is evident that introduction of a methyl group onto the *N*-alkoxy backbone increases the thermal stabilities of the complexes below 200 °C but enhances the pyrolysis rates at the higher temperatures from the variable-temperature TGA data. Even though this cannot be rationalized yet, this property as a potential MOCVD precursor can be exploited for the lower temperature deposition process.

Five Ta(*N*-alkoxy- β -ketoiminate)(OEt)₃ (**2a–e**) and four Nb(*N*-alkoxy- β -ketoiminate)(OEt)₃ (**3a–d**) precursors were tested for the deposition of Ta₂O₅ and Nb₂O₅

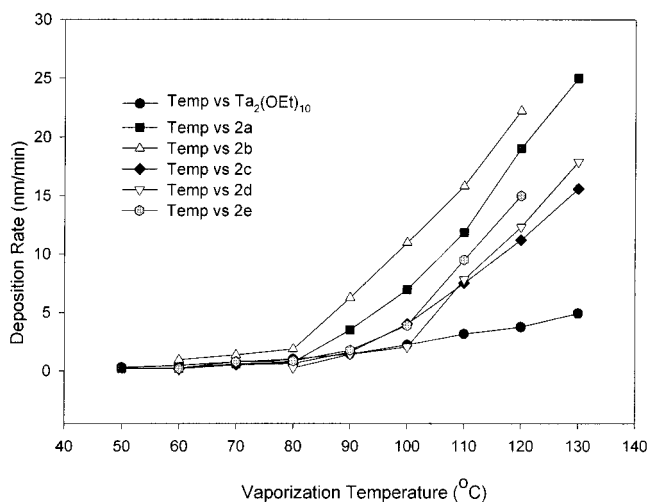


Figure 1. Deposition rates for tantalum oxide films as a function of the vaporization temperature with precursors **2a–e** and Ta₂(OEt)₁₀. (The substrate temperature was 550 °C, and 50 mL/min of N₂ was used for the carrier gas. The mixtures of O₂ and N₂ were used as reaction gases, and their flow rates were 400 and 100 mL/min, respectively.)

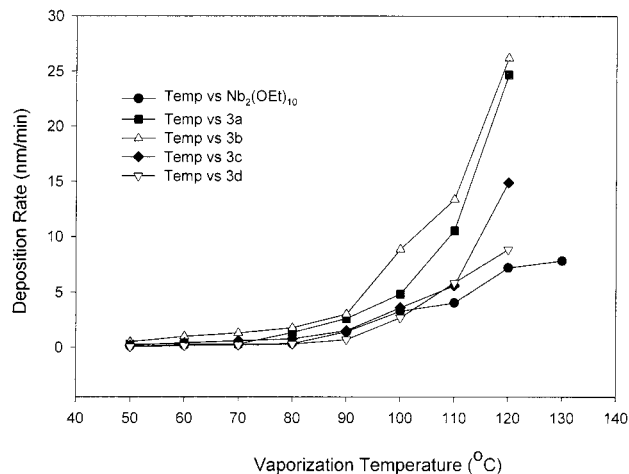


Figure 2. Deposition rates for niobium oxide films as a function of the vaporization temperature with precursors **3a–d** and Nb₂(OEt)₁₀. (The substrate temperature was 550 °C, and 50 mL/min of N₂ was used for the carrier gas. The mixtures of O₂ and N₂ were used as reaction gases, and their flow rates were 400 and 100 mL/min, respectively.)

films. The deposition rates with these precursors are illustrated in Figures 1 and 2. All of the precursors show considerably higher deposition rates than M₂(OEt)₁₀, which is regarded as one of the most popular precursors for Ta₂O₅ and Nb₂O₅ films. In the literature, it is indicated that a typical bubbler temperature for the evaporation of Ta₂(OEt)₁₀ is around 130 °C.^{23,24} The deposition rate of Ta₂O₅ by precursor **2a** is 7 times that of Ta₂(OEt)₁₀, as shown in Figure 1. Therefore, the deposition rate with Ta₂(OEt)₁₀ at 130 °C can be achieved by vaporizing the precursor **2a** only at 95 °C. The same phenomenon was observed in the Nb series (Figure 2). It is worthwhile to point out that the deposition rates of precursors **2b** and **3b**, which have a methyl group in the *N*-hydroxyethyl backbone, are the

(20) Davies, H. O.; Leedham, T. J.; Jones, A. C.; O'Brien, P.; White, A. J. P.; Williams, D. J. *Polyhedron* **1999**, *18*, 3165–3172.

(21) Fleeting, K. A.; O'Brien, P.; Otway, D. J.; White, A. J. P.; Williams, D. J.; Jones, A. C. *Inorg. Chem.* **1999**, *38*, 1432–1437.

(22) Greenwood, N. N.; Earnshaw, A. In *Chemistry of the Elements*; Pergamon Press: New York, 1984; p 1497.

(23) Shinriki, H.; Sugiura, M.; Liu, S.; Shimomura, K. *J. Electrochem. Soc.* **1998**, *145*, 3247.

(24) Lai, B. C.; Lee, J. Y. *J. Electrochem. Soc.* **1999**, *146*, 266.

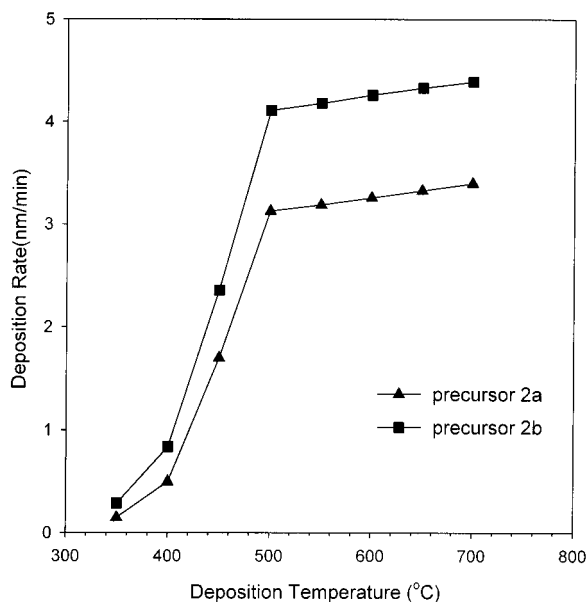


Figure 3. Deposition rates for Ta_2O_5 films as a function of the deposition temperature with precursors **2a** and **2b**. The vaporization temperature was fixed to 100 °C. The flow rate of the carrier gas, N_2 , was 50 mL/min. Mixtures of O_2 and N_2 were used as reaction gases, and their flow rates were 400 and 100 mL/min, respectively.

best among the precursors tested in this study. It is rather surprising that the introduction of only a methyl substituent in the *N*-hydroxyethyl backbone appreciably enhances the deposition rates of Ta_2O_5 and Nb_2O_5 layers. These deposition results are consistent with the trend of the volatility data, which have been estimated as the vacuum distillation temperature for each precursor (**2a**, 144 °C; **2b**, 126 °C; **2c**, 142 °C; **2e**, 140 °C under 10^{-1} Torr; **2d** solid, mp 78 °C; **3a**, 148 °C; **3b**, 128 °C under 10^{-1} Torr; **3c** solid, mp 25 °C; **3d** solid, mp 78 °C). The substitution of a methyl group in the β -ketoiminate backbone with an isopropyl (**2c**) or *tert*-butyl group (**2e**) does not increase the volatility significantly but even decreases the deposition rate. The increased volatility may originate from the dissymmetry of the ligands, which may lower the lattice stabilization energy or interaction of discrete molecules.²⁵ The dissymmetry effect appears to be more pronounced than the bulky ligand effect on the volatility²⁶ in this series of precursors. However, this effect is not significant when the substituents of the β -ketoiminate ligand are isopropyl groups (**2c,d** and **3c,d**), which cannot be explained at present.

The deposition temperature was varied from 500 to 700 °C by fixing the bubbler temperature to 100 °C. The deposition rates as a function of the deposition temperature with precursors **2a** and **2b** are shown in Figure 3. For both precursors, the deposition rates steadily increased up to 500 °C, until it reached a plateau. This suggests that the $\text{Ta}(\text{N-alkoxo-}\beta\text{-ketoiminate})(\text{OR})_3$ precursors are decomposed at a relatively low temperature, compared with the other Ta precursors. Thus, these precursors seem to be good candidates for the fabrication of Ta_2O_5 films at a low temperature.

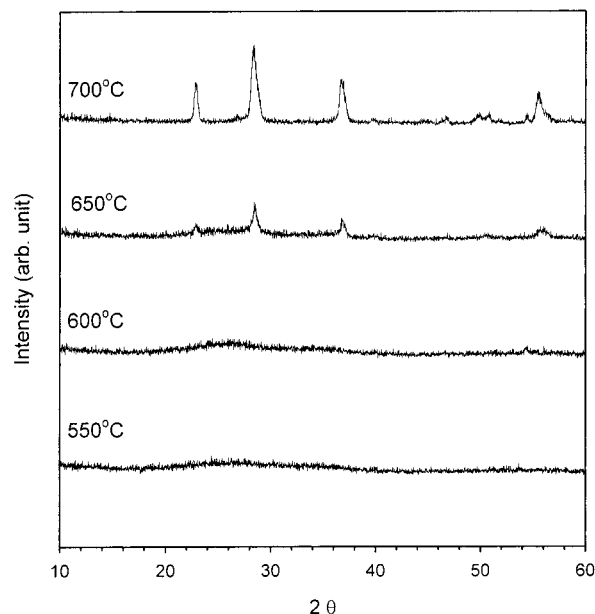


Figure 4. XRD patterns of Ta_2O_5 films deposited at 550–700 °C. The films were grown using precursor **2b**, and their thickness was about 200 nm. XRD patterns were obtained at glancing angle mode (glancing angle: 5°).

The Ta_2O_5 thin films utilized for the X-ray diffraction (XRD), scanning electron microscopy (SEM), Auger electron spectroscopy (AES), and XPS analyses were derived from precursor **2b**. The XRD patterns in Figure 4 indicate that the Ta_2O_5 films are not crystallized until the deposition temperature goes over 650 °C. A typical polycrystalline Ta_2O_5 film in the orthorhombic phase could be obtained by the deposition at 700 °C.

Field emission SEM images of Ta_2O_5 thin films deposited at several substrate temperatures are illustrated in Figure 5. The Ta_2O_5 films deposited at 650 °C or lower than this temperature presented less-crystallized grains having a circular shape. Well-crystallized longish grains were formed in the films deposited at 700 °C, and the grain shape and size in the films were not further changed at higher deposition temperature. The grains in the film were about 120 nm in length and 30 nm in width, and there were no secondary structures. This result is consistent with that obtained by XRD patterns.

The chemical composition and binding energy of Ta in the Ta_2O_5 films deposited at several temperatures were analyzed by AES and XPS, respectively. The thickness of the Ta_2O_5 film used for this experiment was about 200 nm, and the films were deposited with precursor **2b**. Depth profiles of Ta, O, C, and N from the top of the Ta_2O_5 films to the bottom Pt layer are illustrated in Figure 6. For the evaluation of the Ta to O molar ratio, bulk Ta_2O_5 powder was used for the composition calibration. The composition profile of the Ta_2O_5 film deposited at 550 °C is shown in Figure 6a. The nitrogen and carbon impurities were 2.3% and 4.2%, respectively. The relative molar ratio of oxygen to tantalum was 2.18:1.00, which indicated that oxygen was considerably deficient. However, the relative composition among Ta, O, C, and N was not appreciably changed throughout the film depth. The same film was then postannealed at 700 °C in 30 min under an oxygen environment. As is indicated in Figure 6b, the nitrogen

(25) Belot, J. A.; Neumayer, D. A.; Reedy, C. J.; Studebaker, D. B.; Hinds, B. J.; Stern, C. L.; Marks, T. J. *Chem. Mater.* **1997**, *9*, 1638–1648.

(26) Doppelt, P. *Coord. Chem. Rev.* **1998**, *178–180*, 1785–1809.

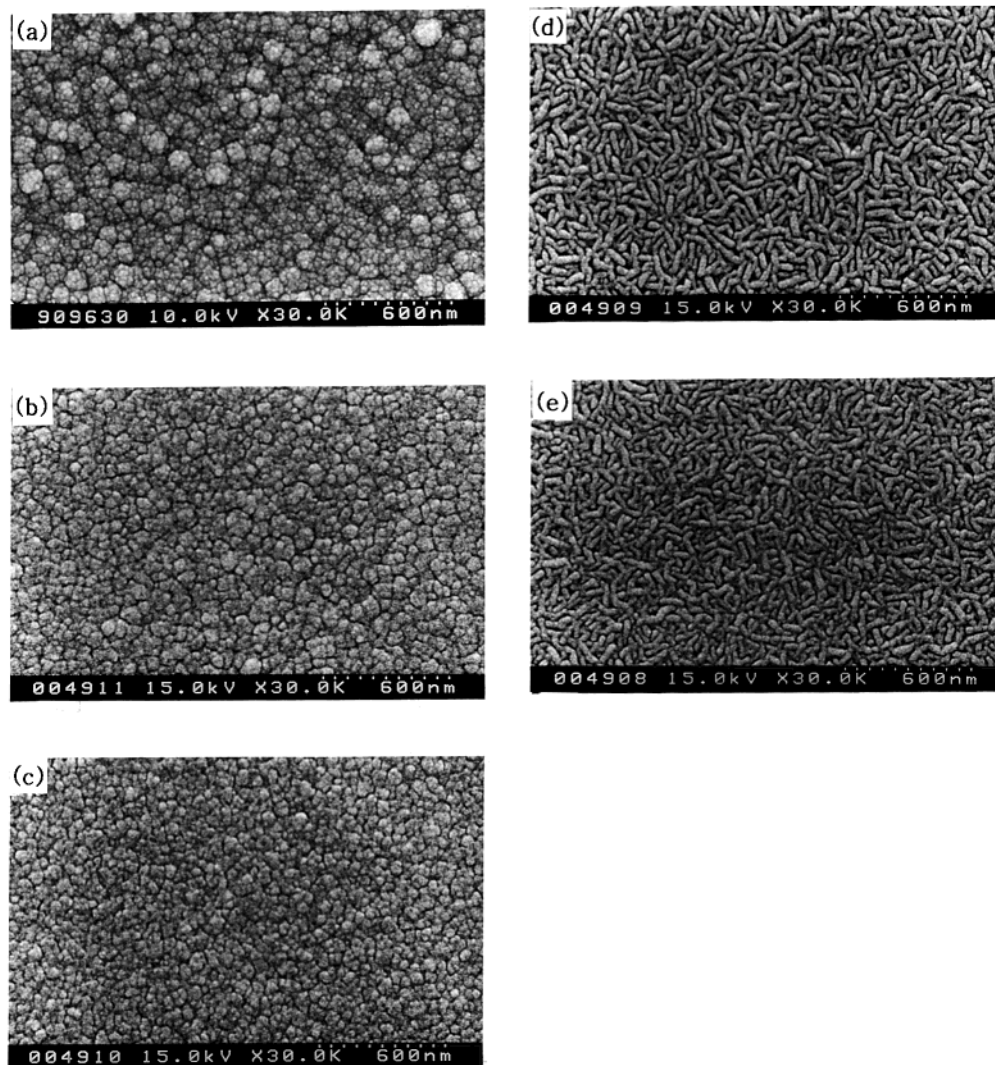


Figure 5. SEM images of Ta_2O_5 films deposited at 550–750 °C. The films were grown using precursor **2b**, and their thickness was about 200 nm. (a) 550 °C, (b) 600 °C, (c) 650 °C, (d) 700 °C, (e) 750 °C.

impurity was completely removed, the carbon residue was negligible (~ 0.5 mol %), and the molar ratio of oxygen to tantalum was 2.35:1.00, which was close to the stoichiometric ratio, 2.5:1.0. Figure 6c presents the depth profile of a Ta_2O_5 film deposited at 700 °C. No nitrogen impurity was found in the film, the residual carbon was 0.4%, and the molar ratio of oxygen to tantalum was 2.45:1.00. The similar results observed between the last two processes indicate that the carbon or nitrogen impurities in Ta_2O_5 films, deposited at a low temperature, are easily removed by the heat treatment at 700 °C in oxygen. It also suggests that for the film deposited at 550 °C the carbon and nitrogen impurities are not incorporated into the Ta_2O_5 structure as carbide or nitride forms.

The binding energy of the Ta $4f_{5/2}$ and $4f_{7/2}$ peaks was analyzed by XPS, as shown in Figure 7. For the Ta_2O_5 films deposited at 550 °C, the position of the $4f_{7/2}$ peak was 25.3 eV. With an increase in the deposition temperature, the position of the Ta $4f_{7/2}$ peak was shifted to higher energy. At 650 °C, the peak position was 26.8 eV, and it was not increased any more by a further increase in the deposition temperature. The low binding energy of the $4f_{7/2}$ peak for the film deposited at 550 °C indicates that the oxidation state of Ta is lower than 5.

It is also indicated that the pure Ta_2O_5 structure can be formed at 650 °C or higher temperature.

Conclusions

$\text{M}(\text{N-Alkoxo-}\beta\text{-ketoiminate})(\text{OEt})_3$ ($\text{M} = \text{Ta}$ and Nb) complexes were successfully prepared by the substitution reaction of $\text{M}_2(\text{OEt})_{10}$ with $\text{N-alkoxo-}\beta\text{-ketoiminates}$ in high yields. These complexes are liquid or low-melting solids and showed enhanced thermal and chemical stability, especially toward moisture. It was confirmed by TGA experiments that the ethoxide ligands decomposed first and then the $\text{N-alkoxo-}\beta\text{-ketoiminate}$ began to decompose in the pyrolysis process. All of the precursors, especially the ones with methyl groups on both the N-alkoxo and $\beta\text{-ketoiminate}$ backbones, demonstrate considerably higher deposition rates than $\text{M}_2(\text{OEt})_{10}$. The XRD patterns indicate that the deposited films are not crystallized until the substrate temperature goes over 650 °C. The composition of the M_2O_5 film was analyzed by XPS and AES depth profiles, which showed that the carbon and nitrogen contaminations in the films deposited at 550 °C are not significant. After heat treatment at 700 °C in oxygen, no nitrogen impurities were found and pure oxide is obtained.

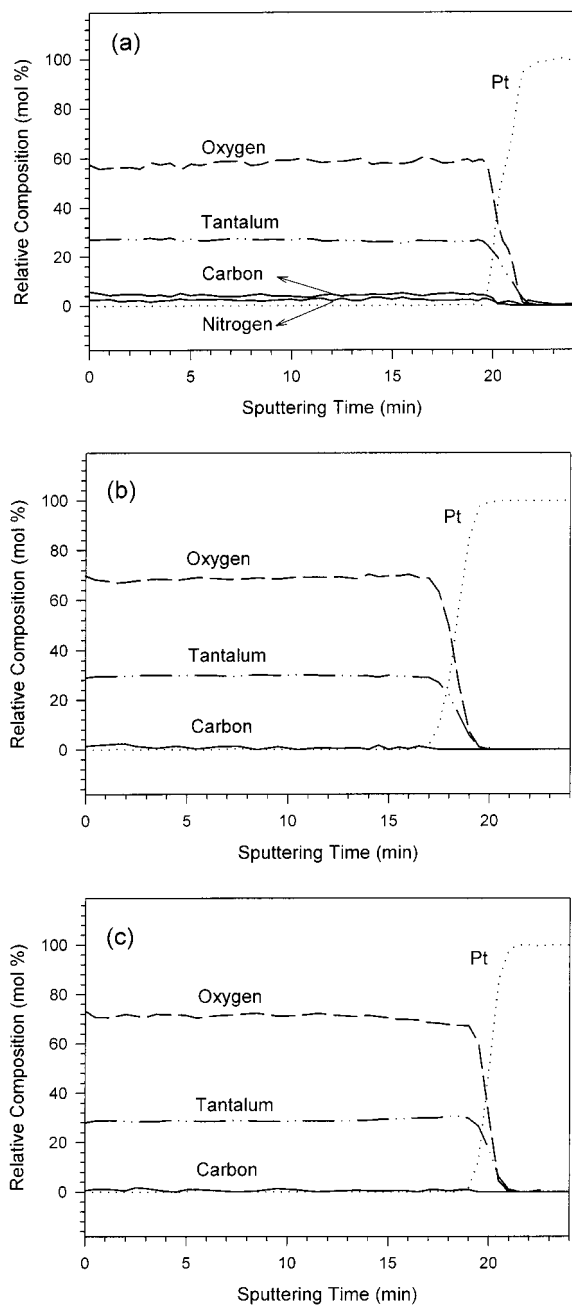


Figure 6. Auger depth profile of Ta_2O_5 films deposited at several conditions. Ta_2O_5 films in 200 nm thickness on Pt layer, grown using precursor **2b**, were in situ sputtered by an Ar^+ beam with a rate of about 8 nm/min. O 1s, C 1s, N 1s, and Ta 4f peaks were used for the composition analyses: (a) as-deposited Ta_2O_5 film at 550 °C; (b) postannealed Ta_2O_5 film at 700 °C for 30 min under oxygen, after it has been deposited at 550 °C; (c) as-deposited Ta_2O_5 films at 700 °C.

Experimental Section

All manipulations were performed under a nitrogen atmosphere using standard Schlenk techniques unless stated otherwise. The solvents were reagent grade and were distilled under nitrogen over appropriate drying agents prior to use. Reagent-grade chemicals were purchased from Aldrich Chemical Co., Inc., and Strem Chemicals Inc. and used without further purification unless stated otherwise. *N*-(Hydroxyalkyl)- β -ketoimines, $\text{CH}_3\text{C}(\text{O})\text{CH}_2\text{C}(\text{NCH}_2\text{CHR}'\text{OH})\text{CH}_3$ [$\text{R}' = \text{H}$ (**1a**); $\text{R}' = \text{Me}$ (**1b**)], were prepared according to published procedures.²⁷ ^1H and ^{13}C NMR spectra were recorded by using a 5 mm tube on a Bruker AC-250 (VT NMR experiments, 250.133

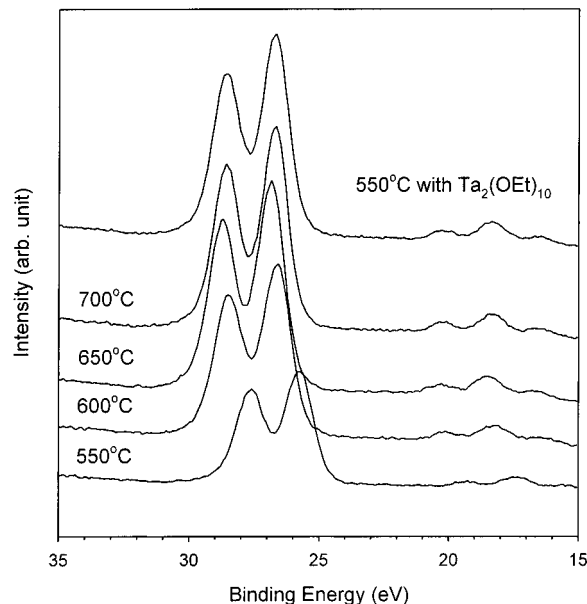


Figure 7. XPS spectra of Ta_2O_5 films deposited at several temperatures. As-deposited films derived from precursor **2b** were used. Ta 4f_{5/2} and Ta 4f_{7/2} peaks were monitored.

and 62.896 MHz, respectively) or Varian Gemini 2000 (RT NMR experiments, 199.976 and 50.289 MHz, respectively) FT NMR spectrometer and were referenced to tetramethylsilane (TMS). Elemental analyses were performed with EA-1110 (CE Instruments) at Inha University. Mass spectral analyses were carried out by employing a gas chromatograph/mass spectrometer (GC/MS; Shimadzu QP5050A).

TGA/DSC was done with NETZSCH STA 449C at Samsung Advanced Institute of Technology.

A laboratory-made cold-wall low-pressure MOCVD apparatus was employed for the testing of the synthesized Ta and Nb precursors in the deposition of Ta_2O_5 and Nb_2O_5 thin films. The graphite susceptor was heated by a radio-frequency induction coil, and the temperature of the bubbler was heat-controlled by an oil bath. The vaporized precursors in the bubbler were delivered to the deposition zone by a N_2 carrier gas with a flow rate of 50 mL/min. For the deposition, the temperature of the susceptor in the reactor was adjusted to 400–700 °C and that of the bubbler was kept at 50–130 °C. Mixtures of O_2 and N_2 were used as reactant gases, and their flow rates were 400 and 100 mL/min, respectively. The substrates used for the deposition of Ta_2O_5 films were Pt/Ti/ SiO_2 /Si. On the Si (100) substrate deposited with 300 nm of SiO_2 , 20 nm of a Ti layer and 220 nm of a Pt layer were sputter-deposited, respectively.

The thicknesses of Ta_2O_5 and Nb_2O_5 films were estimated from the interference fringes obtained by reflectance spectra in the UV–visible region and by the SEM cross section. XPS (SPECS model EA200) was used for the analysis of the composition of Ta_2O_5 and Nb_2O_5 films. Glancing angle mode powder XRD patterns of the metal oxide films were obtained by using a Philips diffractometer (PW3020) with a monochromated high-intensity Cu $K\alpha$ radiation. The surface morphology of M_2O_5 films was observed by a field emission SEM (Hitachi S-4500). AES (Perkin-Elmer PHI-670), and XPS (SPECS model EA200) was used for the analysis of the composition of M_2O_5 films.

Ligand Synthesis. $(\text{CH}_2)_2\text{CHC}(\text{O})\text{CH}_2\text{C}(\text{NCH}_2\text{CH}_2\text{OH})\text{CH}(\text{CH}_3)_2$ (**1c**). Ethanolamine (4.30 g, 70.4 mmol) was added to a solution of toluene (170 mL) containing 2,6-dimethyl-3,5-heptanedione (10.0 g, 64.0 mmol) in a two-necked flask with a Dean–Stark apparatus, and then 1 drop of 98% sulfuric acid

(27) Bertrand, J. A.; Kelley, J. A.; Breece, J. L. *Inorg. Chim. Acta* 1969, 4, 247.

was added to this solution. The resulting solution was refluxed for 3 h. The water produced from the reaction was collected in a trap of the Dean–Stark apparatus. The solution was cooled to room temperature, and the solvent was removed under reduced pressure. The resulting colorless solid was extracted with 100 mL of CH₂Cl₂ three times. Recrystallization from a hexane solution at –20 °C yielded a colorless solid of **1c** in 84.1% yield (10.72 g).

(CH₃)₂CHC(O)CH₂C(NCH₂CHMeOH)CH(CH₃)₂ (1d**).** 1-Amino-2-propanol (5.77 g, 76.8 mmol) and 2,6-dimethyl-3,5-heptanedione (10.0 g, 64.0 mmol) were used to produce **1d** as a colorless solid after recrystallization from a hexane solution at –20 °C in 85.0% yield (11.61 g).

(CH₃)₃CC(O)CH₂C(NCH₂CH₂OH)CH₃ (1e**).** Ethanolamine (9.73 g, 68.4 mmol) and 2,2-dimethyl-3,5-hexanedione (8.11 g, 57.03 mmol) were used to produce **1e** as a colorless solid after recrystallization from a hexane solution at –20 °C in 89.0% yield (9.40 g).

Preparation of Metal Complexes. Ta(1a)(OEt)₃ (2a**).** A solution of **1a** (2.0 g, 13.98 mmol) in 80 mL of toluene was added to a solution of Ta(OEt)₅ (5.16 g, 12.70 mmol) in 40 mL of toluene with rapid stirring. The addition of **1a** was accompanied by the appearance of a pale yellow color. After stirring overnight, the solvent was removed under reduced pressure to leave a yellow liquid residue. This was fractionally distilled under vacuum (144 °C at 10^{–1} Torr) to give **2a** as a yellow liquid in 65.0% yield (3.75 g).

Ta(1b)(OEt)₃ (2b**).** **1b** (2.32 g, 14.8 mmol) and Ta(OEt)₅ (5.00 g, 12.3 mmol) were employed to produce **2b** as a yellow liquid in 57.0% yield (3.02 g). Bp: 126 °C at 10^{–1} Torr.

Ta(1c)(OEt)₃ (2c**).** **1c** (1.61 g, 8.08 mmol) and Ta(OEt)₅ (2.73 g, 6.73 mmol) were employed to produce **2c** as a yellow liquid in 63.0% yield (2.19 g). Bp: 142 °C at 10^{–1} Torr.

Ta(1d)(OEt)₃ (2d**).** **1d** (2.63 g, 12.3 mmol) and Ta(OEt)₅ (5.00 g, 12.3 mmol) were employed to produce **2d** as a pale yellow crystal in 99.8% yield (6.48 g). Mp: 78 °C.

Ta(1e)(OEt)₃ (2e**).** **1e** (1.00 g, 7.03 mmol) and Ta(OEt)₅ (2.85 g, 7.03 mmol) were employed to produce **2e** as a yellow liquid in 72.6% yield (2.33 g). Bp: 140 °C at 10^{–1} Torr.

Nb(1a)(OEt)₃ (3a**).** **1a** (3.24 g, 22.6 mmol) and Nb(OEt)₅ (7.20 g, 22.6 mmol) were employed to produce **3a** as a yellow liquid in 99.8% yield (8.34 g). Bp: 148 °C at 10^{–1} Torr.

Nb(1b)(OEt)₃ (3b**).** **1b** (2.96 g, 18.9 mmol) and Nb(OEt)₅ (5.00 g, 15.7 mmol) were employed to produce **3b** as a yellow liquid in 41.4% yield (2.49 g). Bp: 128 °C at 10^{–1} Torr.

Nb(1c)(OEt)₃ (3c**).** **1c** (3.44 g, 17.3 mmol) and Nb(OEt)₅ (5.00 g, 15.7 mmol) were employed to produce **3c** as a pale yellow solid in 78.0% yield (5.21 g). Mp: 25 °C.

Nb(1d)(OEt)₃ (3d**).** **1d** (3.69 g, 17.3 mmol) and Nb(OEt)₅ (5.00 g, 15.7 mmol) were employed to produce **3d** as a pale yellow solid in 64.9% yield (4.48 g). Mp: 78 °C.

Acknowledgment. This work was supported by the Korea Science and Engineering Foundation (981-0308-047-2) in 1998–1999. The authors thank Yosep Min and Y. T. Kim of Samsung Advanced Institute of Technology for running the TGA experiments.

Supporting Information Available: Elemental analysis, spectroscopic, and TGA data (Table 1) of ligands and complexes prepared in this study are available (PDF). This material is available free of charge via the Internet at <http://pubs.acs.org>.

CM010590F